Thermal performance of an oscillating heat pipe with Al 2O 3–water nanofluids

Article *in* International Communications in Heat and Mass Transfer · February 2010

DOI: 10.1016/j.icheatmasstransfer.2009.10.001

3 authors, including:

Jian Qu
Shanghai Jiao Tong University

Ping Cheng
Shanghai Jiao Tong University

International Communications in Heat and Mass Transfer 37 (2010) 111–115

Contents lists available at ScienceDirect

International Communications in Heat and Mass Transfer

journal homepage: www.elsevier.com/locate/ichmt

Thermal performance of an oscillating heat pipe with Al_2O_3–water nanofluids ☆

Jian Qu, Hui-ying Wu *, Ping Cheng

Key Laboratory for Power Machinery and Engineering of Ministry of Education, School of Mechanical Engineering, Shanghai Jiaotong University, Shanghai 200240, PR China

ARTICLE INFO

Available online 10 November 2009

Keywords:
Oscillating heat pipe
Nanofluids
Nucleate boiling
Heat transfer enhancement
Nanoparticle settlement

ABSTRACT

An experimental investigation was performed on the thermal performance of an oscillating heat pipe (OHP) charged with base water and spherical Al_2O_3 particles of 56 nm in diameter. The effects of filling ratios, mass fractions of alumina particles, and power inputs on the total thermal resistance of the OHP were investigated. Experimental results showed that the alumina nanofluids significantly improved the thermal performance of the OHP, with an optimal mass fraction of 0.9 wt.% for maximal heat transfer enhancement. Compared with pure water, the maximal thermal resistance was decreased by 0.14 °C/W (or 32.5%) when the power input was 58.8 W at 70% filling ratio and 0.9% mass fraction. By examining the inner wall samples, it was found that the nanoparticle settlement mainly took place at the evaporator. The change of surface condition at the evaporator due to nanoparticle settlement was found to be the major reason for the enhanced thermal performance of the alumina nanofluid-charged OHP.

1. Introduction

Technological advances in microelectronic devices with decreasing sizes and increasing heat loads demand for more effective cooling technology. Among them, nanofluids, which are engineered by dispersing metallic/nonmetallic nano-sized particles in base fluids, have received much attention for the past decade [1] due to their enhanced heat transfer capabilities. Recent experimental investigations on convective heat transfer [2,3] and critical heat flux (CHF) [4,5] of nanofluids reaffirmed their tremendous potential for electronic cooling applications.

Heat pipes have been widely used for cooling of electronic devices in recent years. In order to improve the thermal performance of heat pipes, nanofluids have been proposed as working fluids. In 2004, Tsai et al. [6] introduced the water-based gold nanofluids into a circular meshed heat pipe. Their experimental results showed that significant enhancements in the thermal performance of heat pipes were obtained when using the nanofluids instead of the pure water. Subsequently, Kang et al. [7,8] investigated the thermal performance of a micro-grooved circular heat pipe and a sintered heat pipe both charged with the silver nanofluids. They found that although the concentration of nanoparticles was very low (less than 100 ppm), distinguishable lower thermal resistance and evaporator temperature were achieved compared with using pure water. Recently, Naphon et al. [9] performed an experiment in a copper tube heat pipe with alcohol-based titanium nanofluids as working fluids. They found that the thermal efficiency of the heat pipe with a volume fraction of 0.10% nanofluid was enhanced by 10.6% compared with pure alcohol.

Note that all of the aforementioned nanofluid studies were conducted in traditional heat pipes. As a wickless heat pipe, the oscillating heat pipe (OHP) or pulsating heat pipe (PHP) has drawn much attention in the past decade due to its unique features. If the nanofluid is charged into an OHP, the continuous oscillation keeps the nanoparticles from settling and makes them remain suspended. Ma and co-workers [10] have successfully actualized heat transfer enhancement of an OHP charged with nanofluid consisted of HPLC grade water and 1.0% volume fraction of diamond nanoparticles. At the power input of 100 W, they found that the temperature difference between the evaporation and the condensation sections were reduced from 42 °C to 25 °C, which significantly improved the heat transfer capability of the OHP. Similar experiments were also carried out by Lin et al. [11] with water-based silver nanofluid, and considerable heat transfer enhancement was achieved at ultra-low mass fractions.

In this paper, experimental results on the thermal performance of an OHP with water-based Al_2O_3 nanofluids under different mass fractions and filling ratios are reported. To explain the heat transfer enhancement mechanism, both thermal properties owing to the addition of nanoparticles and the change of surface condition due to the nanoparticle deposition on the evaporator are explored. It is found that the change of surface condition of the evaporator because of nanoparticle settlement is mainly responsible for the enhanced heat transfer in an alumina nanofluid-charged OHP.

2. Description of experiment

2.1. Preparation and characterization of nanofluids

The Al_2O_3 nanoparticles with a mean diameter of 56 nm (purchased from Nanophase Techonlogies Corporation) were used as the

☆ Communicated by W.J. Minkowycz.

* Corresponding author.
E-mail address: whysrj@sjtu.edu.cn (H. Wu).

0735-1933/$ – see front matter © 2009 Elsevier Ltd. All rights reserved.
doi:10.1016/j.icheatmasstransfer.2009.10.001

source material, and the pure water was chosen as the base fluid. The water-based alumina nanofluids were synthesized by a two-step method [12]. To avoid the agglomeration of nanopartcles, the electrostatic stabilization method [13] was adopted. For this purpose, the pH values of the base water were regulated by adding small amounts of hydrochloric acid (HCl) solution, and then nanoparticles were added. In order to obtain homogeneous suspension, the dispersion solution was ultrasonic vibrated continuously for 4 h in an ultrasonic bath (SCQ-2210, Shengyan Ultrasonic Equipment Co.). Since the alumina nanoparticles could be stably suspended in water at least for 3 days when the pH value was 4.9, this pH value was chosen in the preparation process. Controlling the pH value and under ultrasonic treatment, alumina nanofluids with five different mass fractions at 0.1%, 0.3%, 0.6%, 0.9% and 1.2% were prepared for this experiment.

2.2. Experimental apparatus and procedure

Fig. 1 illustrates the experimental apparatus composed of an OHP assembly, a multi-channel data acquisition system, a DC power supply unit (GPR-3060D, GW) and a water cold bath (DC-0506, BILANG). The OHP was fabricated by bending a stainless steel capillary tube with an inner diameter of 2 mm and an outer diameter of 3 mm. It had 6 turns with a total length of 3 m. The OHP, consisting of evaporation, adiabatic and condensation sections with 50, 105 and 70 mm in length respectively, was vertically oriented. The evaporation section (evaporator) was electrically heated, and the condensation section (condenser) was cooled by water which pumped from the cold bath. Both the evaporation and adiabatic sections were thermally insulated and the heat loss from these two sections was negligibly small. Sixteen thermocouples with a diameter of 0.1 mm (OMEGA T-type with ± 0.1 °C accuracy) were mounted on the outer surface of the OHP. As illustrated in Fig. 1, eight thermocouples (T_{e1}–T_{e8}) were placed at the evaporator and the other eight (T_{c1}–T_{c8}) thermocouples were located at the condenser. The Agilent 34970A data acquisition system was used to record the experimental data.

Before the experiment, the OHP was evacuated firstly by a vacuum pump, and then it was charged with the nanofluids. The filling ratios were varied at 50%, 60% and 70%. For each filling ratio, the cooling water with constant temperature and flow rate was continuously supplied to the condenser and the power input to the evaporator was stepwise increased. Temperature data at the evaporator and condenser were recorded after the system had reached a steady state condition.

3. Experimental results and discussions

3.1. The overall thermal resistance

The overall thermal resistance (R) is a measure of thermal performance of an OHP, which is defined as

$$R = \frac{\overline{T}_e - \overline{T}_c}{Q} \quad (1)$$

with $\overline{T}_e$ and $\overline{T}_c$ being the average wall temperatures of the evaporator and condenser, respectively. Considering that the heat loss from the evaporation and adiabatic sections of the OHP to the ambience was negligibly small due to good insulation, heating power input, Q, can be evaluated as follows:

$$Q = UI \quad (2)$$

with U and I being the input voltage and current, respectively.

The thermal resistance of the alumina nanofluid-charged OHP, computed from Eq. (1) based on temperature measurements, as a function of the power input was presented in Fig. 2. It can be seen that: (1) the thermal resistance was apparently decreased after the addition of alumina nanoparticles as compared with that of the pure water, i.e., the addition of alumina nanoparticles enhanced the heat transport capability of the OHP; (2) the thermal resistance depended greatly on the filling ratio, and the lower filling ratio led to a smaller thermal resistance; and (3) the thermal resistance decreased with increasing mass fractions of nanoparticles from 0 wt.% (i.e., pure water) to 0.9 wt.%, but it increased when the mass fraction reached 1.2 wt.%. Thus, there was an optimal mass fraction of 0.9 wt.% for minimal thermal resistance or maximal heat transfer performance. At the optimal value of 0.9 wt.%, the maximal decrease of the thermal resistance was about 0.14 °C/W (or 32.5%) as compared with pure water, which occurred at 70% filling ratio when the power input was 58.8 W. Thus, the addition of alumina nanoparticles in the base fluid enhanced the thermal performance of the OHP.

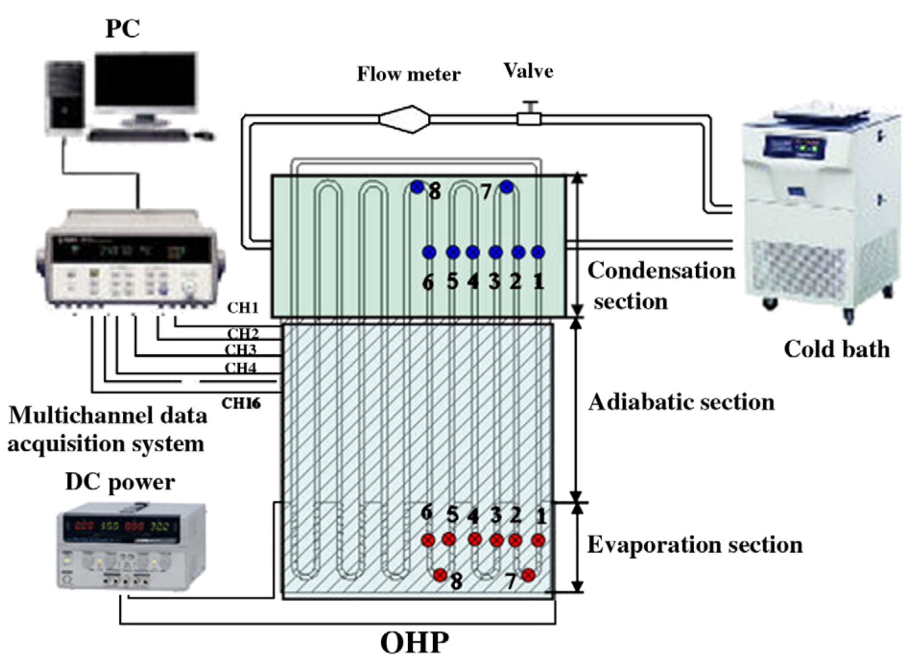

Fig. 1. Experimental apparatus of the oscillating heat pipe.

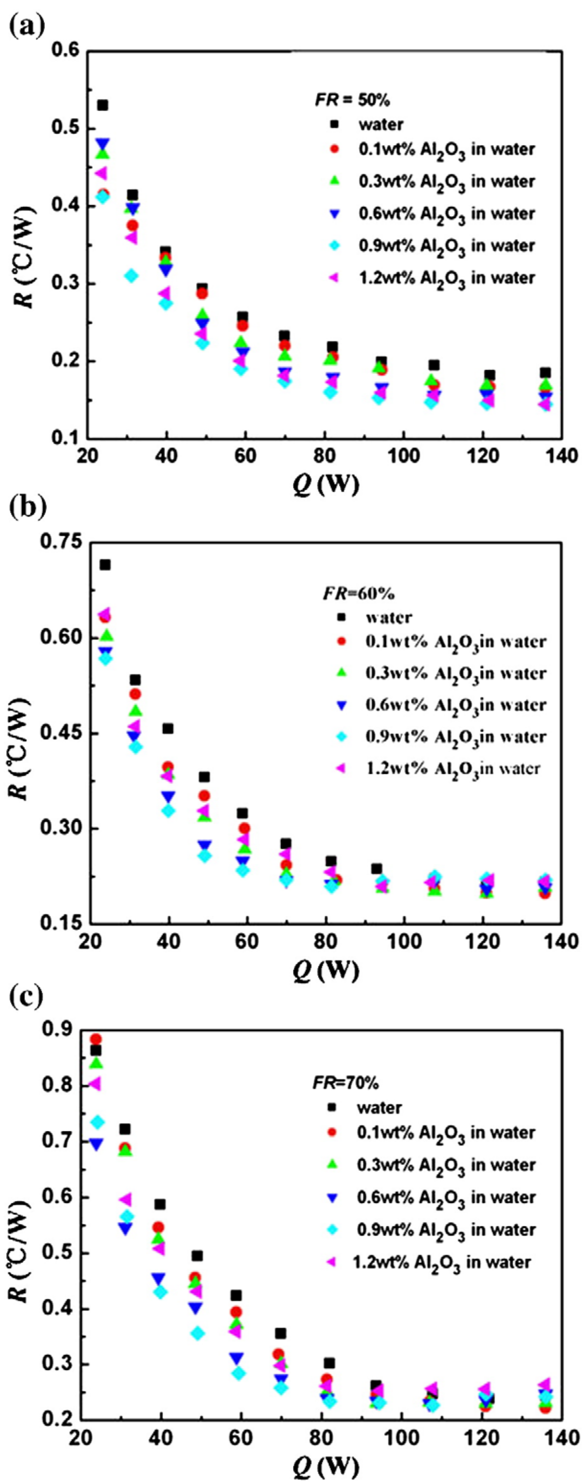

Fig. 2. Thermal resistance comparison for the OHP charged with water and alumina nanofluids at filling ratios of (a) 50%, (b) 60% and (c) 70%.

3.2. Explanation for the heat transfer enhancement of the alumina nanofluid-charged OHP

It is known that the addition of alumina nanoparticles will increase the thermal conductivity of the working fluid and hence the heat transfer capability. However, the increase is small for adding such small mass fractions of nanoparticles (ranging from 0.1 wt.% to 1.2 wt.% in this paper), and it cannot be accounted for the considerable reduction of the thermal resistance as shown in Fig. 2. So it is necessary to analyze the reasons for the reduction of thermal resistance due to other factors. To this end, we note that the overall thermal resistance between the evaporator and condenser of the OHP can be written as follows:

$$R = 2R_{\mathrm{wall}} + R_{\mathrm{l-v}} + R_{\mathrm{evp}} + R_{\mathrm{con}} \tag{3}$$

where R_{wall}, $R_{\mathrm{l\text{-}v}}$, R_{evp} and R_{con} are the conductive thermal resistance in the pipe wall, the thermal resistance in the two-phase flow along the heat pipe length, and the thermal resistances due to boiling/evaporation and condensation at the evaporator and condenser, respectively. Generally, the conductive resistance of a metallic OHP, R_{wall}, is small and is almost independent of the working fluid. Thus, the thermal resistances due to two-phase flow along the heat pipe, $R_{\mathrm{l\text{-}v}}$, the evaporation/boiling at the evaporator, R_{evp}, as well as the condensation at the condenser, R_{con}, in Eq. (3) are the most important factors affecting the thermal performance of an OHP. In the following, we will focus attention on the analysis of nanoparticles on $R_{\mathrm{l\text{-}v}}$, R_{evp}, and R_{con}.

3.2.1. Thermal resistance along the heat pipe length ($R_{l\text{-}v}$)

Although the study of nanofluid two-phase flow (both for boiling and condensation) is rather limited, it is likely that the nanofluids will also enhance the thermal performance of an OHP as compared with the pure water due to the increase of the thermal conductivity. In addition, the oscillation and circulation motion of the working fluid in an OHP keep the nanoparticles suspended, which facilitates nanoparticle migration and prevents sedimentation [10]. Thus, the nanoparticles in the OHP not only increased the fluid thermal conductivity but also enhanced the convective heat transfer due to the particle migration. Consequently, the thermal resistance of the two-phase flow, $R_{\mathrm{l\text{-}v}}$, along the OHP in Eq. (3) would be decreased. However, the decrease of $R_{\mathrm{l\text{-}v}}$ due to the presence of nanoparticles was small because of the relatively small mass fractions of particles. Thus, it is not the main reason for the apparent reduction of the overall thermal resistance in this experiment.

3.2.2. Thermal resistances due to boiling/evaporation and condensation (R_{evp} and R_{con})

Thermal resistances, R_{evp} and R_{con} in Eq. (3) due to boiling/evaporation and condensation, at the evaporator and condenser were greatly influenced by the surface condition. In an OHP, the deposition of nanoparticles may occur both at the evaporator and condenser. In order to analyze the nanoparticle deposition and adhesion effects on the surface condition, representative samples from the evaporator and condenser were obtained by cutting the OHP after the experiments. Besides, a clean sample boiled in pure water was also prepared for comparison. The surface conditions of these three samples were then observed by a scanning electron microscope (S-2150, Hitachi Co.).

Fig. 3 shows the scanning electron microscope (SEM) images of surface conditions of these three samples. Although nanoparticle settlements occurred at both evaporator and condenser, the amount of localized agglomerates at the condenser was negligible as compared with that at the evaporator. Fig. 3(b) shows that the surface condition of the condenser was close to that of a clean surface as shown in Fig. 3(a). So the thermal resistance, R_{con}, due to condensation, was nearly the same for nanofluids and pure water. Therefore, the change of thermal resistance by nanofluids mainly occurred at the evaporator.

Considering that the nucleate boiling prevails at the evaporator of an OHP, the thermal resistance due to nucleate boiling at the evaporator can be written as [14]:

$$R_{\mathrm{evp}} = \frac{1}{2N_{\mathrm{a}}D_{\mathrm{b}}^{2}\sqrt{f}\sqrt{\pi k_{\mathrm{l}}\rho_{\mathrm{l}}c_{\mathrm{l}}}} \tag{4}$$

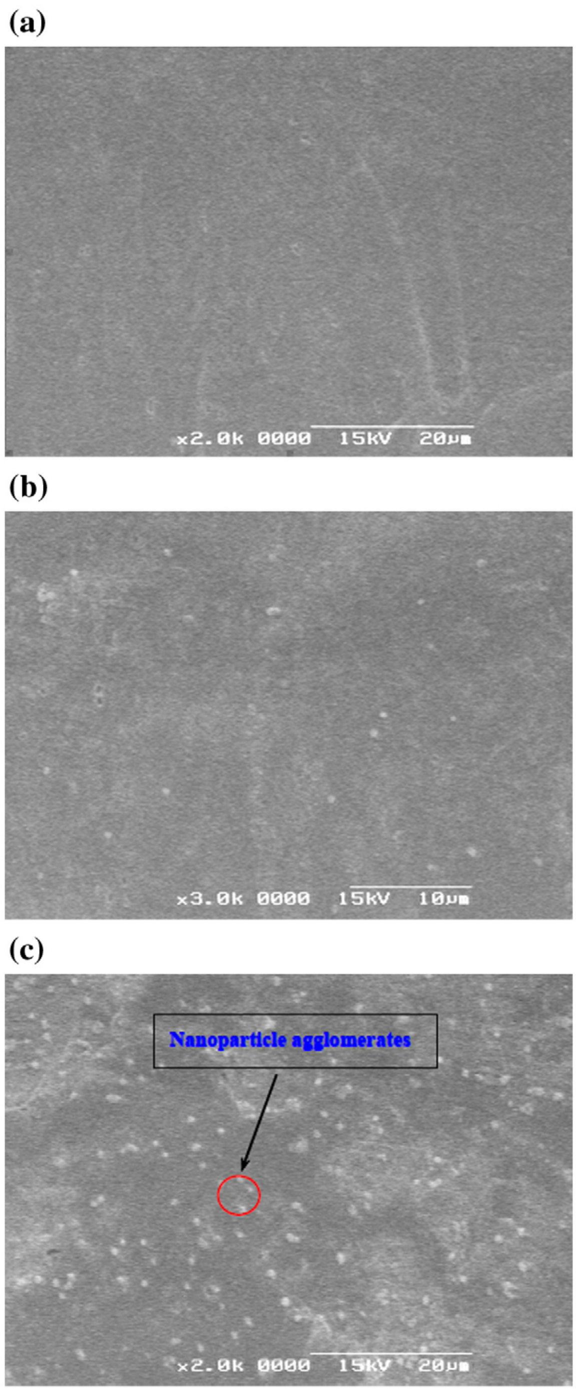

Fig. 3. SEM images of (a) a clean substrate boiled in pure water, (b) a nanoparticle-deposited substrate at the condenser, and (c) a nanoparticle-deposited substrate at the evaporator.

where N_a, D_b, f, k_l, ρ_l and c_l are the active nucleation site density, bubble release diameter, bubble release frequency, liquid thermal conductivity, density and specific heat, respectively. The addition of nanoparticles in the working fluid leads to the increase of the liquid thermal conductivity, k_l, and density, ρ_l, and the decrease of the specific heat, c_l. At the low nanoparticle mass fractions ($\leq$1.2 wt.% in this paper), the variation of the product ($k_l \rho_l c_l$) in Eq. (4) due to the addition of nanoparticles was negligibly small (<1.0%), so their effects on the R_{evp} were negligible. Thus, the effects of nanoparticles on the changes in the values of N_a, D_b and f are more important for the change in R_{evp}.

Generally, the active nucleation site density N_a is related to the surface condition and roughness. Fig. 4(a) and (b) show the 2D atomic force microscope (Multimode Nanoscope IIIa, Digital Instrument) images of the surface morphology for clean substrate and alumina nanoparticle-deposited substrate of the evaporator respectively. As can be seen from Fig. 4(b), the alumina nano-structure completely modified the surface of the evaporator. The cavities of the clean surface were on the magnitude of about 2–3 μm as shown in Fig. 4(a), so they were one or two orders of magnitude larger than the size of nanoparticles deposited on the evaporator surface. As a result, when the smaller nanoparticles sit on nucleation sites, they can create more new active nucleation sites by splitting a single nucleation site into multiple ones (i.e., N_a is increased), and enhance the boiling heat transfer [15].

In addition, the irregular nanopores formed between the deposited alumina nanoparticles which created the nano-roughness within the micrometer-roughened surface would affect the bubble release diameter and frequency. The bubble generation on the nano-microroughened hierarchical surface was different from that of a clean surface. Within the cavities through the nanopore network, the nanobubbles may be continuously generated and feed the nucleation and growth of larger bubbles at the microscale cavities [16]. This enables stable nucleation with increasing bubble release frequency f. Although the bubbles with smaller size D_b may be created on the hierarchical surface which plays a negative role for the reduction of

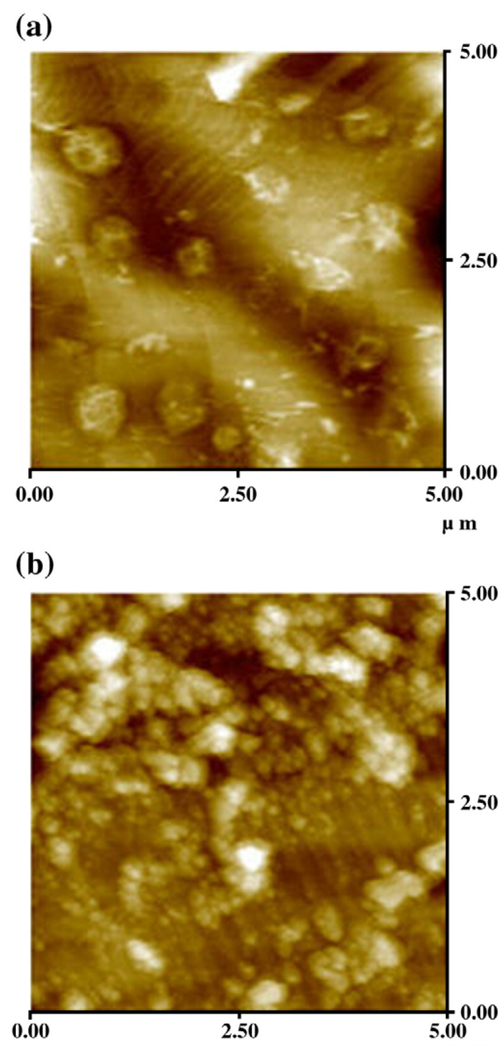

Fig. 4. 2D atomic force microscope images of (a) a clean substrate boiled in pure water and (b) a nanoparticle-deposited substrate at the evaporator.

thermal resistance as seen from Eq. (4), the dramatic increase of the active nucleation site density N_a and the release frequency f will overwhelmingly intensify the boiling performance and decrease the thermal resistance of the evaporator. Thus the decrease of R_{evp} is mainly responsible for the heat transfer enhancement of the alumina nanofluid-charged OHP.

Note that the level of particle agglomerate is basically enhanced by increasing the mass fraction. However, if the size of nanoparticles exceeds a certain value, the nucleation sites will decrease from the peak, and then leads to the degradation of the boiling performance. Consequently, an optimal mass fraction of the nanoparticles for the maximal thermal performance as demonstrated in Fig. 2 existed.

4. Conclusions

An experimental investigation was conducted for the thermal performance of a stainless steel oscillating heat pipe, which was charged with water-based alumina nanofluids. The following conclusions can be drawn:

(1) The heat transfer performance of an OHP was apparently improved after the addition of alumina nanoparticles in the working fluid. Compared with the pure water, the maximal decrease of thermal resistance was 0.14 °C/W (or 32.5%) which occurred at 70% filling ratio and 0.9% mass fraction when the power input was 58.8 W.

(2) 0.9% was the optimal mass fraction of the alumina nanofluids to achieve the maximal heat transfer enhancement of the OHP for the filling ratios at 50%, 60% and 70%.

(3) The nanoparticle settlement mainly took place at the evaporator. The change of the surface condition at the evaporator was mainly responsible for the heat transfer enhancement of the nanofluid-charged OHP.

Acknowledgments

This work was supported by the National Natural Science Foundation of China though Grant No. 50925624, the Program for New Century Excellent Talents in University of China through Grant No. NCET-06-0406, and Shanghai Municipal Education Commission through Grant Nos. 08ZZ10 and 08GG05. The authors would also like to thank the Instrumental Analysis Center of Shanghai Jiaotong University for their helps in the analysis and measurement of experimental samples.

References

[1] S.K. Das, S. Choi, H. Patel, Heat transfer in nanofluids — a review, Heat Transfer Engineering 27 (2006) 3–19.
[2] Y. Xuan, Q. Li, Investigation on convective heat transfer and flow features of nanofluids, ASME Journal of Heat Transfer 125 (2003) 151–155.
[3] S.Z. Heris, M.N. Esfahany, S.G. Etemad, Experimental investigation of convective heat transfer of Al_2O_3/water nanofluid in circular tube, International Journal of Heat and Mass Transfer 28 (2007) 203–210.
[4] S.M. You, J.H. Kim, K.H. Kim, Effect of nanoparticles on critical heat flux of water in pool boiling heat transfer, Applied Physics Letters 83 (2003) 3374–3376.
[5] I.C. Bang, S.H. Chang, Boiling heat transfer performance and phenomena of Al_2O_3–water nano-fluids from a plain surface in a pool, International Journal of Heat and Mass Transfer 48 (2005) 2407–2419.
[6] C.Y. Tsai, H.T. Chien, B. Chan, P.H. Chen, P.P. Ding, T.Y. Luh, Effect of structural character of gold nano-particles in nanofluid on heat pipe thermal performance, Materials Letters 58 (2004) 1461–1465.
[7] S.W. Kang, W.C. Wei, S.H. Tsai, S.Y. Yang, Experimental investigation of silver nano-fluid on heat pipe thermal performance, Applied Thermal Engineering 26 (2006) 2377–2382.
[8] S.W. Kang, W.C. Wei, S.H. Tsai, C.C. Huang, Experimental investigation of nanofluids on sintered heat pipe thermal performance, Applied Thermal Engineering 29 (2009) 973–979.
[9] P. Naphon, P. Assadamongkol, T. Borirak, Experimental investigation of titanium nanofluids on the heat pipe thermal efficiency, International Communications in Heat and Mass Transfer 35 (2008) 1316–1319.
[10] H.B. Ma, C. Wilson, B. Borgmeyer, K. Park, Q. Yu, S. Choi, M. Tirumala, Effect of nanofluid on the heat transport capability in an oscillating heat pipe, Applied Physics Letters 88 (2006) 143116.
[11] Y.H. Lin, S.W. Kang, H.L. Chen, Effect of silver nano-fluid on pulsating heat pipe thermal performance, Applied Thermal Engineering 28 (2008) 1312–1317.
[12] C.H. Li, G.P. Peterson, The effect of particle size on the effective thermal conductivity of Al_2O_3–water nanofluids, Journal of Applied Physics 101 (2007) 044312.
[13] X.F. Li, D.S. Zhu, X.J. Wang, N. Wang, J.W. Gao, H. Li, Thermal conductivity enhancement dependent pH and chemical surfactant for Cu–H_2O nanofluids, Thermochimica Acta 469 (2008) 98–103.
[14] B.B. Mikic, W.M. Rohsenow, A new correlation of pool-boiling data including the effect of heating surface characteristics, Journal of Heat Transfer 91 (1969) 245–250.
[15] S.K. Das, G.P. Narayan, A.K. Baby, Survey on nucleate pool boiling of nanofluids: the effect of particle size relative to roughness, Journal of Nanoparticle Research 10 (2008) 1099–1108.
[16] C. Li, Z. Wang, P. Wang, Y. Peles, N. Koratkar, G.P. Peterson, Nanostructured copper interface for enhanced boiling, Small 4 (2008) 1084–1088.